

## Somatic mutation-associated T follicular helper cell elevation in lung adenocarcinoma

Kevin W Ng<sup>a</sup>, Erin A Marshall<sup>a,b</sup>, Katey SS Enfield<sup>a,b</sup>, Spencer D Martin<sup>a,b</sup>, Katy Milne<sup>c</sup>, Michelle E Pewarchuk<sup>a</sup>, Ninan Abraham<sup>d,e</sup>, and Wan L Lam<sup>a,b</sup>

<sup>a</sup>British Columbia Cancer Research Centre, Integrative Oncology Department, Vancouver, Canada; <sup>b</sup>Faculty of Medicine, University of British Columbia, Vancouver, Canada; <sup>c</sup>Deeley Research Centre, Victoria, Canada; <sup>d</sup>Department of Microbiology and Immunology, University of British Columbia, Vancouver, Canada; <sup>e</sup>Department of Zoology, University of British Columbia, Vancouver, Canada

### ABSTRACT

T follicular helper cells (Tfh) play crucial roles in the development of humoral immunity. In the B cell-rich germinal center of lymphoid organs, they select for high-affinity B cells and aid in their maturation. While Tfh have known roles in B cell malignancies and have prognostic value in some epithelial cancers, their role in lung tumour initiation and development is unknown. Through immune cell deconvolution, we observed significantly increased Tfh in tumours from two independent cohorts of lung adenocarcinomas and found that this upregulation occurs early in tumour development. A subset of tumours were stained for T and B cells using multicolour immunohistochemistry, which revealed the presence of tumour-adjacent tertiary lymphoid organs in 17/20 cases each with an average of 16 Tfh observed in the germinal center. Importantly, Tfh levels were correlated with tumour mutational load and immunogenic cancer testis antigens, suggesting their involvement in mounting an active immune response against tumour neoantigens.

### ARTICLE HISTORY

Received 26 February 2018  
Revised 16 July 2018  
Accepted 17 July 2018

### KEYWORDS

T follicular helper cell; tertiary lymphoid organ; lung adenocarcinoma; neoantigen; CT antigen

### Introduction

The selection of B cells that produce high-affinity antibodies depends on T follicular helper cells (Tfh), antigen-experienced CD4 + T cells that migrate to B cell zones in lymphoid tissue following antigen presentation.<sup>1,2</sup> In these germinal centres, Tfh select for high affinity B cells by providing survival and proliferation signals and ultimately guide the diversity of B cell receptors.<sup>1,3</sup> Beyond their role in the germinal centre reaction, Tfh deregulation and dysfunction have been shown to influence infection, autoimmune disease, and both solid and hematologic tumours.<sup>1</sup> Though the study of Tfh function and dynamics has primarily focused on secondary lymphoid organs, this germinal centre reaction is recapitulated in tertiary lymphoid organs (TLOs).

TLOs are transient structures formed under conditions of chronic inflammation that functionally and structurally resemble secondary lymphoid organs, including the full spectrum of Tfh function.<sup>4</sup> In addition to sites of chronic infection and autoimmune disease, TLOs have been detected in a range of solid cancer types, including lung, breast, colorectal, and skin, where they mediate antitumour immunity via CD8 + T cell and antibody-based cytotoxicity.<sup>4</sup> The presence and density of TLOs correlate with favourable patient outcome in the vast majority of primary and metastatic tumours investigated, though the role of TLO-specific Tfh remains poorly defined.<sup>4</sup>

In lung cancer, follicular B cell and dendritic cell density independently correlate with favourable overall and

recurrence-free survival.<sup>5,6</sup> Mechanistically, this antitumour effect is associated with the activation of B cell maturation machinery and presence of tumour antigen-specific antibodies.<sup>6</sup> Despite the well-characterized role of infiltrating B cells and TLOs, the role of Tfh in human lung cancers remains understudied.<sup>7</sup> Infection models have revealed that circulating Tfh function differently from those in lymphoid tissue and correlate with opposing outcomes.<sup>8</sup> In human breast cancers and mouse models of colorectal cancer, increased Tfh correlates with increased survival.<sup>9,10</sup>

Mutated cancer antigens, or neoantigens, have emerged as critical targets of the antitumour immune response. Increased neoantigen loads have been associated with improved responses to checkpoint blockade in cancers, and neoantigen specific T cells have been isolated in patients responding to immune checkpoint inhibitors.<sup>11</sup> The role of neoantigen-specific CD4 + T cells in guiding anti-tumour immunity has been demonstrated, but due to the extensive *ex vivo* T cell expansion required to identify these cells, the original phenotypes of the CD4 + T cells are lost. The role that CD4+ Tfh cells play in orchestrating the neoantigen-specific antitumour immune response has yet to be investigated.

Here, we assess Tfh dynamics and identify potential immunological targets in human lung tumour tissue through integration of transcriptomic and histologic data. We identify elevation of Tfh in tumour tissue through *in silico* deconvolution of microdissected tumour-derived gene expression

profiles against known Tfh-specific signatures compared to matched non-malignant tissue and validate these findings in two external cohorts of lung adenocarcinoma, as well as through direct immunohistochemical staining of stromal tertiary lymphoid organs. We identify Tfh elevation as an early event in human lung tumour development. Additionally, we establish an association of Tfh levels with nonsynonymous mutational load and with immunogenic cancer testis antigen expression.

## Methods

### Patient samples

83 pairs of fresh frozen lung adenocarcinoma (LUAD) tumours and adjacent non-malignant tissue were obtained from the BC Cancer Agency (BCCA) under written, informed consent approved by the UBC/BCCA Research Ethics Boards. Histological sections were reviewed by a lung pathologist and microdissected to > 80% tumour cell content as previously described.<sup>12</sup> Total RNA was extracted using Trizol reagent (ThermoFisher, MA) and gene expression profiles were generated using the Illumina WG6 microarrays.

### Immune cell deconvolution

Relative immune cell fractions were enumerated from BCCA, The Cancer Genome Atlas (TCGA), and Stage I LUAD datasets using CIBERSORT.<sup>13</sup> Outliers were identified and removed via nonlinear regression followed by false discovery correction (FDR-BH  $p < 0.01$ ).<sup>14</sup>

### Immunohistochemistry

In order to confirm the immune cell patterns in our primary cohort obtained through deconvolution, formalin fixed paraffin embedded (FFPE) tumour tissues from 20 among the 83 patients described above were cut into 4  $\mu\text{m}$ -thick sections. Sections were baked at 37°C overnight and deparaffinized. Antigen retrieval was performed using decloaking chamber plus with Diva decloaker (Biocare). Automated blocking (peroxidized-1, background sniper 1) and first round staining (Panel 1: anti-CD3 (SP7/Spring Biosciences), anti-CD8 (C8/144B/Sigma-Aldrich), Panel 2: anti-PD1 (NAT105/Abcam), anti-PD-L1 (SP142/Spring Biosciences), DaVinci Green diluent, Mach2 Double Stain #2, Ferenghi Blue, DAB) was performed within a Intellipath FLX rack. Slides were removed, rinsed with  $\text{dH}_2\text{O}$ , incubated in SDS-glycine pH2.0 for 45 minutes at 50°C, and rinsed with  $\text{dH}_2\text{O}$ .<sup>15</sup> Slides were returned to the Intellipath FLX racks for automated staining with Mouse AP polymer, Warp Red chromogen, and CAT hematoxylin counter stain. Second round staining included Panel 1: anti-CD79a (SP18/Spring Biosciences) or Panel 2: anti-CD8 (C8/144B/Sigma-Aldrich), DaVinci Green diluent, Mouse-AP polymer, Warp Red chromogen, and 1:5 dilution of CAT hematoxylin counterstain. Images were analyzed using a Panoramic Digital Slide Scanner from 3D Histotech and the Panoramic Viewer software. 4–5 8000  $\times$  8000 pixel regions were investigated per tissue section for a total of 93 regions analyzed. Each region was independently evaluated in triplicate

for immunohistological quantification of tertiary lymphoid organs and T follicular helper cells.

### Validation cohorts

Gene expression profiles from unmatched LUAD and non-malignant lung tissues were obtained from The Cancer Genome Atlas (TCGA) ( $n_{\text{tumour}} = 517$ ,  $n_{\text{normal}} = 59$ ), and matched samples from the LUAD Stage I cohort ( $n_{\text{tumour}} = n_{\text{normal}} = 32$ , GSE63459).<sup>16</sup> The expression profiles for the TCGA cohort were generated using the Agilent 244K custom gene expression G4502A\_07\_3 microarray,<sup>17</sup> while the profiling of the matched LUAD Stage I cohort used the Illumina HumanRef-8 v3.0 expression beadchip.<sup>16</sup> For all single gene expression comparisons, outliers were identified and removed via nonlinear regression followed by false discovery correction (FDR-BH  $p < 0.01$ ).<sup>14</sup> For heatmaps, hierarchical clustering by Euclidean distance was performed on Z-score-normalized gene expression values.

## Results

### Tfh are elevated in tumour tissue

Advances in gene expression profiling and *in silico* immunological techniques have enabled the elucidation of the infiltrating immune profile of solid tumours. Thus, we analyzed tumour and normal tissue gene expression data from a cohort of 83 matched lung adenocarcinomas (LUAD) and paired non-malignant lung tissue. In order to identify the immune cell types most significantly enriched in tumour tissue, expression profiles were analyzed using CIBERSORT, a deconvolution algorithm that infers relative cell content of 22 immune cell types.<sup>13</sup> Tumour enrichment of cell types was measured by fold change in tumour versus non-malignant lung tissue. The most dramatically increased immune cell subsets were regulatory T cells (Tregs) (mean fold change (FC) = 9.21), naive macrophages (M0) (mean FC = 5.11), and T follicular helper cells (Tfh) (FC = 4.33) (Figure 1A). Expression of plasma cell markers were also found to be increased in tumour samples compared to normal (FC = 2.87) (Figure 1A). While Tregs and M0 macrophages have been extensively described in lung cancer,<sup>18,19</sup> Tfh cells remains relatively understudied.

To validate our finding that Tfh expression signatures were significantly upregulated in lung cancers, we analyzed expression signatures of Tfh in an independent cohort of LUAD (TCGA,  $n = 576$ ). Using the same analysis pipeline, we found that Tfh expression signatures were significantly elevated in tumours compared to normals (FC = 3.28) (Figure 1B). Hierarchical clustering based on the 57 CIBERSORT Tfh signature genes was able to separate tumours from non-malignant samples in the matched BCCA cohort (Figure 1C). Expression of *PDCD1* and *CXCR5*, encoding PD1 and CXCR5, were elevated in tumour tissue in both cohorts (Fig S1). These genes are specifically weighted to Tfh cells in the CIBERSORT LM22 signature and are commonly used to define Tfh populations by flow cytometry.<sup>13</sup> Of note, *BCL6*, encoding the defining transcription factor for Tfh

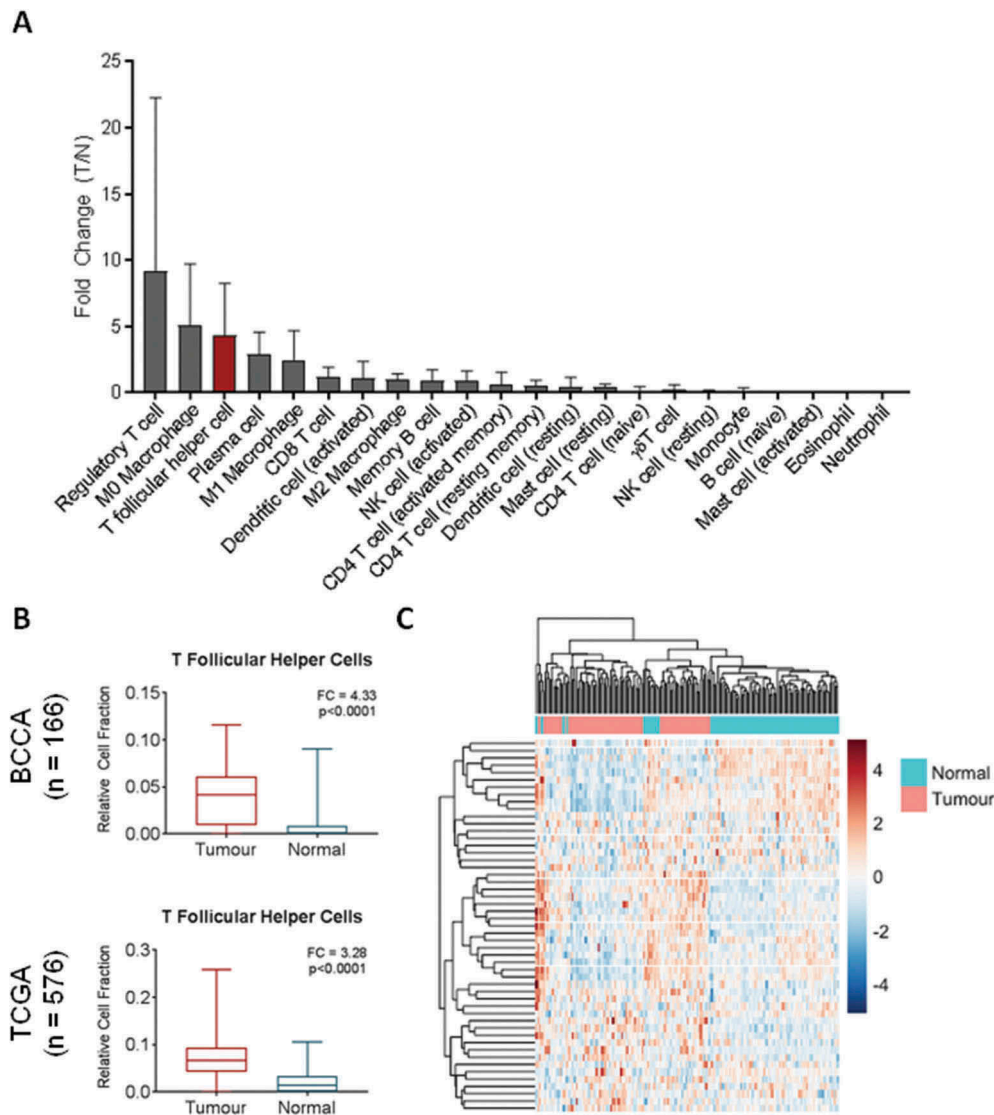


**Figure 1. Relative expression of immune cell subsets in bulk gene expression data.** A) CIBERSORT was used to deconvolve cell fractions of 22 immune cell subsets in matched tumour ( $n = 83$ ) and normal ( $n = 83$ ) samples, and the tumour to normal ratio of each cell type was calculated per each matched pair and the mean across the cohort calculated. B) Relative cell fraction of T follicular helper cells (Tfh) in bulk expression data from BCCA ( $n_{\text{tumour}} = 83$ ,  $n_{\text{normal}} = 83$ ) was compared using a Wilcoxon sign-rank test and validated in the TCGA unpaired cohort ( $n_{\text{tumour}} = 517$ ,  $n_{\text{normal}} = 59$ , Mann Whitney U test). C) Unsupervised hierarchical clustering of tumour (pink) and normal (turquoise) tissues from BCCA based on row-normalized expression of Tfh signature genes (blue = low expression, red = high expression). All boxplots display the median value, with 25th to 75th percentile values denoted by the box and minimum and maximum values by the error bars.

differentiation, showed no elevation in tumour tissue nor did *TCF7* (encoding TCF1), *PRDM1* (BLIMP-1), or *ICOS* (ICOS) (Fig S1), all of which have been shown to regulate Tfh differentiation via *BCL6* and other key transcription factors.<sup>20,21</sup> *ICOS* was in fact reduced in tumour tissue, possibly due to the transient and temporally-specific nature of ICOS-dependent Tfh promotion in the TLO.<sup>21</sup> In summary, in two independent lung cancer cohorts, we found that expression signatures of Tfh cells were upregulated in tumours and that expression of Tfh signature genes was able to distinguish tumours from non-malignant tissue.

#### **Tfh are associated with B cell activation and plasma cells**

Given the critical role of Tfh cells in the activation and maturation of B cells and the potential for plasma B cells to play a key role in antitumour immunity, we next

investigated relative levels of B cell expression signatures in the two cohorts. We found that plasma cells were significantly elevated in tumour tissue compared to normal tissue in both cohorts (Figure 2A). Tfh also play an active role in facilitating differentiation of memory B cells – however, no increase in memory subsets was observed in tumour tissue in the BCCA cohort (Fig S2). Additionally, when we divided the cohort into high, intermediate and low Tfh expression levels, we found that relative fraction of plasma cells increased proportionally with Tfh levels in both cohorts, suggesting a possible linkage between the two cell types (Figure 2B). In support of the presence of an active B cell response, we noted increased tumour expression of *BATF*, a transcription factor that regulates B cell class-switch recombination and Tfh differentiation.<sup>22</sup> Expression was elevated in tumour tissue in both cohorts (Fig S3), consistent with an active germinal centre response.

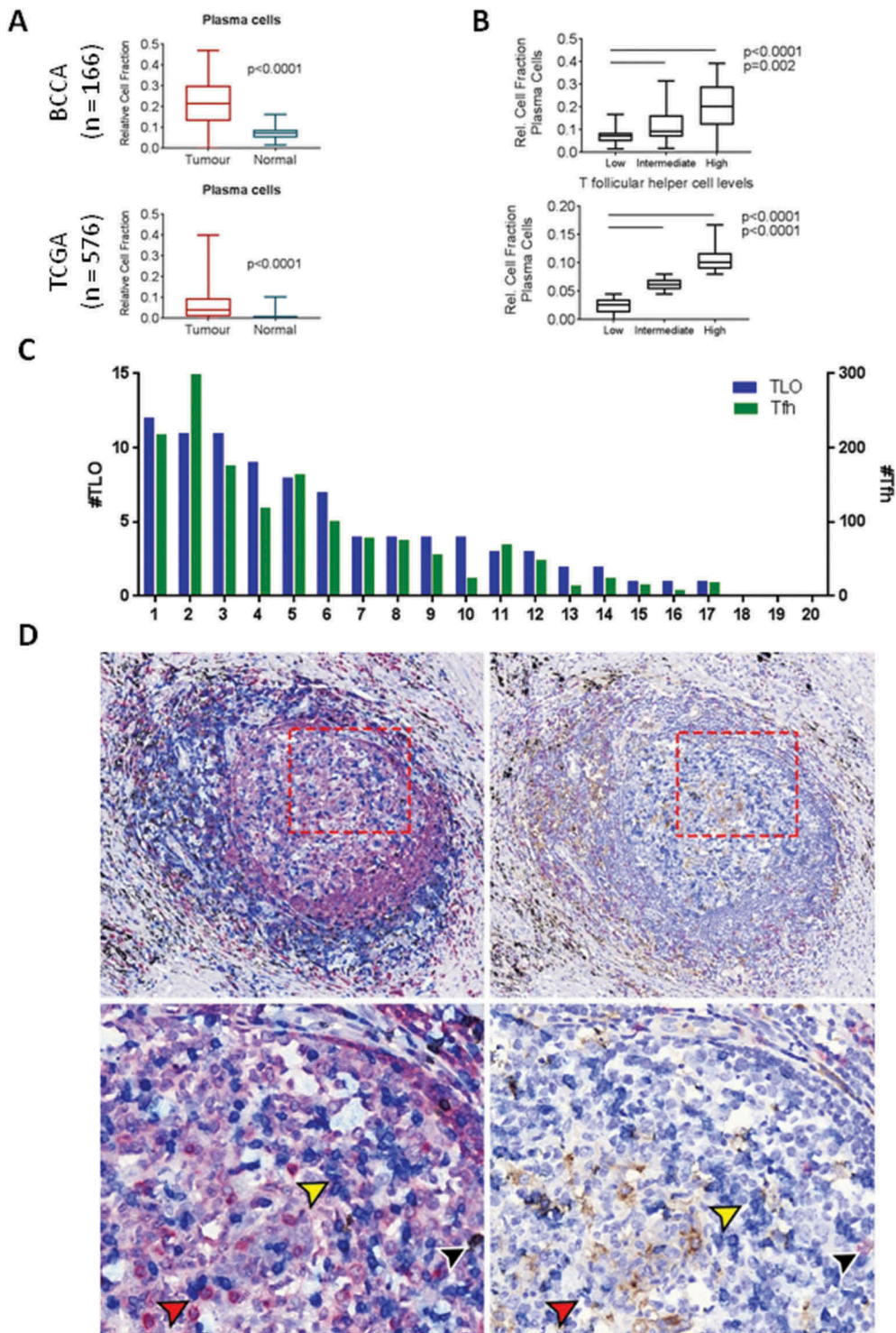


**Figure 2. T follicular helper cells are associated with plasma cells and are present in the germinal center of tertiary lymphoid organs.** A) The relative cell fraction of plasma cells in bulk expression data from BCCA ( $n_{\text{tumour}}=83$ ,  $n_{\text{normal}}=83$ ) was compared using a paired t-test ( $p < 0.0001$ ) and validated in the TCGA unpaired cohort ( $n_{\text{tumour}}=517$ ,  $n_{\text{normal}}=59$ ,  $p < 0.0001$ ). B) Relative cell fraction of plasma cells in relation to T follicular helper cell (Tfh) fraction was assessed by stratification of TCGA tumours into tertiles according to Tfh fraction. C) Quantification of tertiary lymphoid organs (blue, left Y axis) and Tfh (green, right Y axis) across 20 tumour sections from BCCA. D) Immunohistochemistry images of serial sections stained for: (left panels) CD79a (red), CD3 (blue), CD8 (brown), and counterstained with haematoxylin, and (right panels) CD8 (red), PD1 (blue), PD-L1 (brown), and counterstained with haematoxylin. Yellow arrows indicate CD3+ PD1+ cells (blue stain, both panels); black arrows indicate CD3+ CD8+ PD1+ cells (blue and brown stain (left), red stain (right)); red arrows indicate areas of adjacent CD3+ and CD79a+ cells (left panel) as well as adjacent PD1+ and PD1- cells (right panel). Upper images: 10x magnification, lower images 20x magnification. All boxplots display the median value, with 25th to 75th percentile values denoted by the box and minimum and maximum values by the error bars.

Thus, we found that the increased expression signature of Tfh was associated with activated B cell responses, potentially providing a mechanism for increased anti-tumour humoral activity.

### TLOs are common within lung adenocarcinoma

Tfh are important to the formation and function of TLOs, including those found in the stroma of solid cancers.<sup>1</sup> To assess whether Tfh and TLO were active in lung cancers, we performed immunohistological analysis for T and B cells on a representative subset of tumours (n = 20) from the BCCA discovery cohort.<sup>23</sup> Each section was stained using multiplex immunohistochemistry for CD79a (B cells), CD3 (T cells), and CD8 (cytotoxic T cells), and 4–5 immune-dense regions per section investigated for a total of 93 regions analyzed. For our analysis, Tfh were defined as CD3+ CD8- T cells identified in the follicular zone of TLOs. TLO were defined as lymphoid aggregates containing separate but adjacent B and T cell zones; we verified the structural similarity of TLOs with lymph nodes stained with the same protocol, and immune-dense regions with no discernible germinal centre structure were excluded from this analysis (Fig S4A). We found that 17 of 20 full tumour sections contained at least one TLO, with a mean of 4.4 TLOs per section (Figure 2C). We quantified the number of Tfh (follicular CD3+ CD8-) per sample, with a mean of 75.7 Tfh per section and 15.6 Tfh per TLO (Figure 2C, indicated by black arrows in Fig S4A). As expected, the number of Tfh correlated with TLO size (Fig S4B). Importantly, direct cell-to-cell contact between T and B cells were frequently observed by histology in the germinal

centre light zone (Figure 2D), suggesting active facilitation of B cell responses in tumours. This was consistent with our *in silico* results showing association between expression of Tfh and plasma cell markers. We verified that these CD3+ CD8- cells stained positive for PD1 in adjacent sections, providing further evidence that these are *bona fide* Tfh (Figure 2D). The observation of increased plasma cell presence within bulk tumour expression profiles as well as the presence of TLOs in the majority of LUAD samples provides a potential link between Tfh and plasma cells within the LUAD microenvironment.

### Tfh infiltrate early in tumour development and correlates with somatic mutational burden

Understanding the temporal dynamics of adaptive immune responses to tumours at different stages may provide insight into the tumour components that are recognized by the immune system. Thus, we assessed Tfh and plasma cell marker expression through tumour progression by stratifying the TCGA LUAD dataset (n = 576) according to tumour stage. Tfh signatures were increased in Stage I tumours and remained constantly elevated in Stage I-IV (Figure 3A). Similarly, the plasma cell signature was consistently upregulated in Stage I tumours compared to normals and remained constant with increasing stage (Figure 3A), consistent with our previous observations of coordinated elevation of Tfh and plasma cells. Similar results were observed in an additional cohort of 32 Stage I LUAD with matched non-malignant profiles (Fig S5).<sup>16</sup>

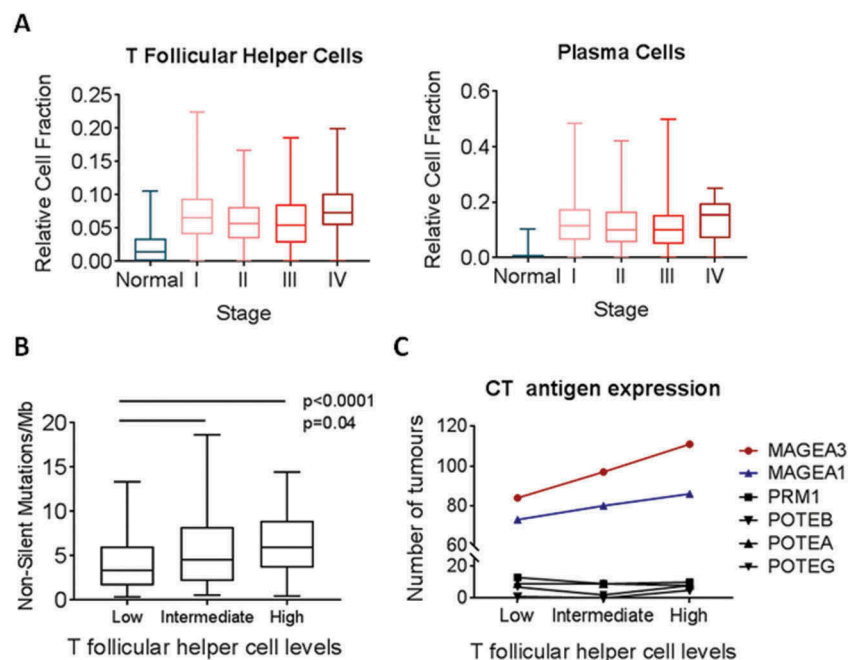


**Figure 3. Relative fraction of T follicular helper cells by tumour stage and mutation burden across TCGA tumours.** A) Relative cell fraction of T follicular helper cells (Tfh) was assessed in relation to tumour stage and compared to normal lung. B) Tumors were stratified into tertiles according to Tfh fraction, and quantification of non-silent mutations per megabase was assessed in relation to Tfh fraction (n = 275). C) Each tumor was assessed as either expressing or not six CT antigens. The number of tumors within each tertile that expressed the immunogenic CT antigens MAGEA1 and MAGEA3 and the non-x-chromosome CT antigens PRM1, POTEb, POTEa, and POTEg was assessed (n = 576). All boxplots display the median value, with 25th to 75th percentile values denoted by the box and minimum and maximum values by the error bars.

Adaptive immune responses are known to occur early in and throughout tumourigenesis in response to tumour-associated antigens and neoantigens.<sup>24</sup> In order to explore the association of Tfh with neoantigen load, we analyzed a subset of tumours (n = 275) with characterized somatic mutational loads.<sup>17</sup> When stratified by Tfh levels, the number of non-silent somatic mutations per megabase increased significantly with Tfh signatures (Figure 3B). Since increased mutational load may identify tumours with specific mutational drivers, we assessed whether Tfh expression associated with *KRAS* or *EGFR* status, common driver mutations in NSCLC with heterogeneous immune infiltration patterns.<sup>25</sup> Interestingly, there was no significant difference of Tfh levels in tumours bearing mutated *KRAS* or *EGFR* compared to those with wild-type *KRAS* or *EGFR* (Fig S6), suggesting that Tfh recruitment relates to the number of mutations rather than specific driver mutations.

We also assessed the association of Tfh with MAGE-A and MAGE-A3 (Figure 3C), immunogenic cancer testis (CT) antigens in NSCLC towards which T cell responses have been detected.<sup>26,27</sup> We found that tumours with the highest levels of Tfh were more likely to express the CT antigens MAGE-A1 and MAGE-A3, while the overall cancer testis antigen expression levels did not change (Fig S7). Conversely, CT antigens that had not previously been described to elicit T cell reactivity were not upregulated in Tfh high tumours. These data support the hypothesis that Tfh may initiate or augment anti-tumour immunity against specific immunogenic proteins such as CT antigens.

## Discussion

Therapeutic interest in the capacity of antibodies to restrain tumour growth combined with increased spatial understanding of immune cells in the tumour microenvironment has drawn interest to the pivotal role of Tfh. Indeed, various systems-based analyses have highlighted Tfh as key modulators of the immune landscape across cancer types.<sup>10,13</sup> Here, we establish that Tfh are elevated in LUAD tissue and correlate with elevated plasma cells in TLOs. Furthermore, elevated levels of Tfh can be observed in Stage I tumours, and correspond to increased mutational burden and immunogenic CT antigen expression.

*In silico* deconvolution techniques have enabled large-scale retrospective analysis of the cellular content of tumours and other pathologies. However, such analyses can be skewed by the presence of cell types omitted from the signature file, particularly in the case of highly heterogeneous tumour types. Thus, validation of such analyses must be carefully considered. We opted for a histology-based approach as it allowed us to analyze the same samples we used for the *in silico* analysis, and because it enabled us to investigate the spatial structure and organization of lymphocytes within the tumour microenvironment. Accordingly, the presence of T cells in the follicular zone of tumour-adjacent TLOs allowed us to directly visualize T-B cell interactions *in situ*, which would not have been possible with flow cytometry. Our report of elevated Tfh in tumours by histology is corroborated by a recently-published single-cell transcriptomic analysis of 14 non-small-cell lung tumours, which revealed an increase of CXCL13<sup>hi</sup> CD4 + T cells in tumour tissue

compared to matched non-malignant lung tissue or peripheral blood from the same patient.<sup>28</sup>

TLOs have emerged as critical structures of interest in cancer immunology, having been observed in a variety of solid tumour types including lung.<sup>5,29</sup> Though the presence and density of TLOs have been found to correlate with better patient outcomes across tumour types,<sup>4</sup> further investigation into their mechanism of antitumour immunity as well as drivers of their formation is warranted. In particular, the role that TLO B cells play in anti-tumour immunity has been understudied. Studies have demonstrated that B cells can have either a pro- or anti-tumour effect, based in part on their developmental stage and isotype.<sup>30</sup> Indeed, a recent scRNAseq analysis of five non-small-cell lung tumours identified B cells as the most tumour-enriched stromal cell type, with approximately a threefold increase in tumours compared to non-malignant tissue from a distal region within the same lobe; within this fraction, follicular (CD20+ CXCR4+ HLA-DR+) and plasma (IgG+) cells were particularly enriched, supporting our findings.<sup>31</sup> Given the well-described mechanism by which Tfh control the regulation of germinal center B cells, we speculate that Tfh cells may play key roles in determining the pro- versus anti-tumour effects of intratumoural B cells. Tfh also play an active role in facilitating differentiation of memory B cells – however, no increase in memory subsets was observed in tumour tissue in the BCCA cohort (Fig S2), possibly due to their migration to the periphery.<sup>32</sup> Recent reports have implicated IL-6 in germinal centre formation via increased differentiation of CD4 + T cells into a Tfh phenotype.<sup>33</sup> Given the pro- and anti-tumoural role of IL-6 in lung cancer, TLO formation may represent yet another function of this pleiotropic molecule through modulation of the tumour microenvironment as well as on tumour cells themselves.<sup>34,35</sup>

Stratification by tumour stage revealed that Tfh elevation occurs even in early-stage lung adenocarcinoma. Furthermore, the observed association between Tfh levels and non-silent mutational load suggests that the presence of tumour neoantigens may drive recruitment and aggregation of Tfh and TLO. Indeed, a study that examined lung TLOs in secondary tumours derived from various primary sites showed higher TLO density in metastases derived from highly mutated melanoma, lung, and prostate cancers compared to less mutated renal and breast cancers,<sup>29</sup> suggesting neoantigens play a major role initiating TLO responses.<sup>24</sup> Antibodies may bind altered surface proteins resulting from such neoantigens, and high affinity, neoantigen-specific TCR on Tfh may induce B cell maturation and Ig class switching. Given that successful anti-PD1 therapy is associated with neoantigen load, we speculate that Tfh may be central players in neoantigen-specific antitumour immunity. Similarly, the association between high Tfh levels and tumour expression of the CT antigens MAGE-A1 and MAGE-A3 suggests Tfh may augment CT antigen-specific immunity. These mechanisms may amplify the anti-tumour immune response by integrating the activity of T, B, and NK cells through antibody-directed cell cytotoxicity.<sup>36</sup> Due to the high expression of PD1 on Tfh cells, the effects of anti-PD1 therapy on Tfh function may have implications for immunotherapeutic success and warrants further investigation.

## Acknowledgments

The authors would like to acknowledge Dr. John English, Adam Sage, and Brenda Minatel for helpful discussion and critical appraisal of the manuscript.

## Author contributions

KWN, EAM, and KSSE conceived and designed the project, performed data analysis, and prepared the manuscript. SDM, MEP, and NA contributed to data interpretation and manuscript preparation. KM contributed to acquisition of data. WLL is the principal investigator of this project. All authors approved the final manuscript.

## Disclosure statement

No potential conflict of interest was reported by the authors.

## Funding

This work was supported by a grant from the Canadian Institutes for Health Research (CIHR FDN – 143345, MOP-126060) and Canadian Graduate Scholarships to E.A.M. and K.S.S.E. E.A.M. is also a Vanier Canada Graduate Scholar.

## Acronyms

BCL6	B Cell CLL/Lymphoma 6
CXCR5	C-X-C Motif Chemokine Receptor 5
FFPE	Formalin-fixed paraffin-embedded
ICOS	Inducible T Cell Costimulator
LUAD	Lung adenocarcinoma
M0	Uncommitted macrophage
PDCD1	Programmed Cell Death Protein 1
PRDM1	Positive Regulatory Domain I-Binding Factor 1
TCF7	T Cell Factor 7
TCGA	The Cancer Genome Atlas
Tfh	T follicular helper cell
TLO	Tertiary lymphoid organ
Treg	Regulatory T cell

## References

- Crotty S. T follicular helper cell differentiation, function, and roles in disease. *Immunity*. 2014;41:529–542. doi:10.1016/j.immuni.2014.10.004.
- Shulman Z, Gitlin AD, Targ S, Jankovic M, Pasqual G, Nussenzweig MC, Victora GD. T follicular helper cell dynamics in germinal centers. *Science*. 2013;341:673–677. doi:10.1126/science.1241680.
- Victora GD, Schwickert TA, Fooksman DR, Kamphorst AO, Meyer-Hermann M, Dustin ML, Nussenzweig MC. Germinal center dynamics revealed by multiphoton microscopy with a photoactivatable fluorescent reporter. *Cell*. 2010;143:592–605. doi:10.1016/j.cell.2010.10.032.
- Dieu-Nosjean MC, Goc J, Giraldo NA, Sautes-Fridman C, Fridman WH. Tertiary lymphoid structures in cancer and beyond. *Trends Immunol*. 2014;35:571–580. doi:10.1016/j.it.2014.09.006.
- Dieu-Nosjean MC, Antoine M, Danel C, Heudes D, Wislez M, Poulot V, Rabbe N, Laurans L, Tartour E, de Chaisemartin L, Lebecque S. Long-term survival for patients with non-small-cell lung cancer with intratumoral lymphoid structures. *J Clin Oncol*. 2008;26:4410–4417. doi:10.1200/JCO.2007.15.0284.
- Germain C, Gnjatic S, Tamzalit F, Knockaert S, Remark R, Goc J, Lepelley A, Becht E, Katsahian S, Bizouard G, et al. Presence of B cells in tertiary lymphoid structures is associated with a protective immunity in patients with lung cancer. *Am J Respir Crit Care Med*. 2014;189:832–844. doi:10.1164/rccm.201309-1611OC.
- Jones GW, Hill DG, Jones SA. Understanding immune cells in tertiary lymphoid organ development: it is all starting to come together. *Front Immunol*. 2016;7:401. doi:10.3389/fimmu.2016.00401.
- Schultz BT, Teigler JE, Pissani F, Oster AF, Kranias G, Alter G, Marovich M, Eller MA, Dittmer U, Robb ML, et al. Circulating HIV-specific interleukin-21(+)CD4(+) T cells represent peripheral Tfh cells with antigen-dependent helper functions. *Immunity*. 2016;44:167–178. doi:10.1016/j.immuni.2015.12.011.
- Gu-Trantien C, Loi S, Garaud S, Equeter C, Libin M, de Wind A, Ravoet M, Le Buanec H, Sibille C, Manfouo-Foutsop G, Veys I, et al. CD4(+) follicular helper T cell infiltration predicts breast cancer survival. *J Clin Invest*. 2013;123:2873–2892. doi:10.1172/JCI67428.
- Bindea G, Mlecnik B, Tosolini M, Kirilovsky A, Waldner M, Obenauf AC, Angell H, Fredriksen T, Lafontaine L, Berger A, et al. Spatiotemporal dynamics of intratumoral immune cells reveal the immune landscape in human cancer. *Immunity*. 2013;39:782–795. doi:10.1016/j.immuni.2013.10.003.
- Goodman AM, Kato S, Bazhenova L, Patel SP, Frampton GM, Miller V, Stephens PJ, Daniels GA, Kurzrock R. Tumor mutational burden as an independent predictor of response to immunotherapy in diverse cancers. *Mol Cancer Ther*. 2017;16:2598–2608. doi:10.1158/1535-7163.MCT-17-0386.
- Becker-Santos DD, Thu KL, English JC, Pikor LA, Martinez VD, Zhang M, Vucic EA, Luk MT, Carraro A, Korbek J, et al. Developmental transcription factor NFIB is a putative target of oncofetal miRNAs and is associated with tumour aggressiveness in lung adenocarcinoma. *J Pathol*. 2016;240:161–172. doi:10.1002/path.4765.
- Gentles AJ, Newman AM, Liu CL, Bratman SV, Feng W, Kim D, Nair VS, Xu Y, Khuong A, Hoang CD, et al. The prognostic landscape of genes and infiltrating immune cells across human cancers. *Nat Med*. 2015;21:938–945. doi:10.1038/nm.3909.
- Motulsky HJ, Brown RE. Detecting outliers when fitting data with nonlinear regression - a new method based on robust nonlinear regression and the false discovery rate. *BMC Bioinformatics*. 2006;7:123. doi:10.1186/1471-2105-7-123.
- Pirici D, Mogoanta L, Kumar-Singh S, Pirici I, Margaritescu C, Simionescu C, Stanescu R. Antibody elution method for multiple immunohistochemistry on primary antibodies raised in the same species and of the same subtype. *J Histochem Cytochem*. 2009;57:567–575. doi:10.1369/jhc.2009.953240.
- Robles AI, Arai E, Mathé EA, Okayama H, Schetter AJ, Brown D, Petersen D, Bowman ED, Noro R, Welsh JA, et al. An integrated prognostic classifier for stage I lung adenocarcinoma based on mRNA, microRNA, and DNA methylation biomarkers. *J Thoracic Oncol*. 2015;10:1037–1048. doi:10.1097/JTO.0000000000000560.
- Comprehensive molecular profiling of lung adenocarcinoma. *Nature*. 2014;511:543–550. doi:10.1038/nature13385.
- Conway EM, Pikor LA, Kung SHY, Hamilton MJ, Lam S, Lam WL, Bennewith KL, et al. Macrophages, inflammation, and lung cancer. *Am J Respir Crit Care Med*. 2016;193:116–130. doi:10.1164/rccm.201508-1545CI.
- Marshall EA, Ng KW, Kung SHY, Conway EM, Martinez VD, Halvorsen EC, Rowbotham DA, Vucic EA, Plumb AW, Becker-Santos DD, et al. Emerging roles of T helper 17 and regulatory T cells in lung cancer progression and metastasis. *Mol Cancer*. 2016;15:67. doi:10.1186/s12943-016-0551-1.
- Xu L, Cao Y, Xie Z, Huang Q, Bai Q, Yang X, He R, Hao Y, Wang H, Zhao T, et al. The transcription factor TCF-1 initiates the differentiation of T(FH) cells during acute viral infection. *Nat Immunol*. 2015;16:991–999. doi:10.1038/ni.3229.
- Stone EL, Pepper M, Katayama CD, Kerdiles YM, Lai CY, Emslie E, Lin YC, Yang E, Goldrath AW, Li MO, et al. ICOS coreceptor signaling inactivates the transcription factor FOXO1 to promote Tfh cell differentiation. *Immunity*. 2015;42:239–251. doi:10.1016/j.immuni.2015.01.017.
- Ise W, Kohyama M, Schraml BU, Zhang T, Schwer B, Basu U, Alt FW, Tang J, Oltz EM, Murphy TL, et al. The transcription factor

- BATF controls the global regulators of class-switch recombination in both B cells and T cells. *Nat Immunol.* 2011;12:536–543. doi:10.1038/ni.2037.
23. Enfield KSS, Kung SHY, Gallagher P, Milne K, Chen Z, Piga D, Lam S, English J, Guillaud M, Macaulay C, et al. P2.01-065 Quantification of tumor-immune cell spatial relationships in the lung tumor microenvironment using single cell profiling. *J Thorac Oncol.* 2017;12:S826–S827. doi:10.1016/j.jtho.2016.11.1117.
  24. Alexandrov, LB., Nik-Zainal S, Wedge DC, Aparicio SA, Behjati S, Biankin AV, Bignell GR, Bolli N, Borg A, Borresen-Dale AL, Signatures of mutational processes in human cancer. *Nature.* 2013;500:415–421. doi:10.1038/nature12477.
  25. Chen Z, Fillmore CM, Hammerman PS, Kim CF, Wong KK. Non-small-cell lung cancers: a heterogeneous set of diseases. *Nat Rev Cancer.* 2014;14:535–546. doi:10.1038/nrc3775.
  26. Djureinovic D, Hallström BM, Horie M, Mattsson JSM, La Fleur L, Fagerberg L, Brunnström H, Lindskog C, Madjar K, Rahnenführer, et al. Profiling cancer testis antigens in non-small-cell lung cancer. *JCI Insight.* 2016;1:e86837. doi:10.1172/jci.insight.86837.
  27. Chiriva-Internati M, Pandey A, Saba R, Kim M, Saadeh C, Lukman T, Chiaramonte R, Jenkins M, Cobos E, Jumper C, et al. Cancer testis antigens: a novel target in lung cancer. *Int Rev Immunol.* 2012;31:321–343. doi:10.3109/08830185.2012.723512.
  28. Guo X, Zhang Y, Zheng L, Zheng C, Song J, Zhang Q, Kang B, Liu Z, Jin L, Xing R. Global characterization of T cells in non-small-cell lung cancer by single-cell sequencing. *Nat Med.* 2018;24:978–985. doi:10.1038/s41591-018-0045-3.
  29. Remark R, Alifano M, Cremer I, Lupo A, Dieu-Nosjean M-C, Riquet M, Crozet L, Ouakrim H, Goc J, Cazes A, et al. Characteristics and clinical impacts of the immune environments in colorectal and renal cell carcinoma lung metastases: influence of tumor origin. *Clin Cancer Res.* 2013;19:4079–4091. doi:10.1158/1078-0432.CCR-12-3847.
  30. Zitvogel L, Kroemer G. Cancer: antibodies regulate antitumor immunity. *Nature.* 2015;521:35–37. doi:10.1038/nature14388.
  31. Lambrechts D, Wauters E, Boeckx B, Aibar S, Nittner D, Burton O, Bassez A, Decaluwé H, Pircher A, Van den Eynde K, et al. Phenotype molding of stromal cells in the lung tumor microenvironment. *Nat Med.* 2018. doi:10.1038/s41591-018-0096-5.
  32. Shinnakasu R, Inoue T, Kometani K, Moriyama S, Adachi Y, Nakayama M, Takahashi Y, Fukuyama H, Okada T, Kurosaki T. Regulated selection of germinal-center cells into the memory B cell compartment. *Nat Immunol.* 2016;17:861–869. doi:10.1038/ni.3460.
  33. Arkatkar T, Du SW, Jacobs HM, Dam EM, Hou B, Uckner JH, Rawlings DJ, Jackson SW. B cell-derived IL-6 initiates spontaneous germinal center formation during systemic autoimmunity. *J Exp Med.* 2017;214:3207–3217. doi:10.1084/jem.20170580.
  34. Qu, Z, Sun F, Zhou J, Li L, Shapiro SD, Xiao G.. Interleukin-6 prevents the initiation but enhances the progression of lung cancer. *Cancer Res.* 2015;75:3209–3215. doi:10.1158/0008-5472.CAN-14-3042.
  35. Caetano MS, Zhang H, Cumpian AM, Gong L, Unver N, Ostrin EJ, Daliri S, Chang SH, Ochoa CE, Hanash S, et al. IL6 blockade reprograms the lung tumor microenvironment to limit the development and progression of K-ras-mutant lung cancer. *Cancer Res.* 2016;76:3189–3199. doi:10.1158/0008-5472.CAN-15-2840.
  36. Ferris RL, Lenz H-J, Trotta AM, García-Foncillas J, Schulten J, Audhuy F, Merlano M, Milano G. Rationale for combination of therapeutic antibodies targeting tumor cells and immune checkpoint receptors: harnessing innate and adaptive immunity through IgG1 isotype immune effector stimulation. *Cancer Treat Rev.* 2017;63:48–60. doi:10.1016/j.ctrv.2017.11.008.